AIAA JOURNAL
Vol. 41, No. 6, June 2003

Nonlinear Vibrations of Circular Cylindrical Shells with Different Boundary Conditions

Marco Amabili*
Università di Parma, 43100 Parma, Italy

Large-amplitude (geometrically nonlinear) vibrations of circular cylindrical shells with different boundary conditions and subjected to radial harmonic excitation in the spectral neighborhood of the lowest resonances are investigated. In particular, simply supported shells with allowed and constrained axial displacements at the edges are studied; in both cases, the radial and circumferential displacements at the shell edges are constrained. Elastic rotational constraints are assumed; they allow simulating any condition from simply supported to perfectly clamped, by varying the stiffness of this elastic constraint. Two different nonlinear, thin shell theories, namely Donnell's and Novozhilov's theories, are used to calculate the elastic strain energy. The formulation is also valid for orthotropic and symmetric cross-ply laminated composite shells. Geometric imperfections are taken into account. Comparison of calculations to experimental and numerical results available in the literature is performed. Both empty and fluid-filled shells are investigated by using a potential fluid model. The nonlinear equations of motion are studied by using a code based on arclength continuation method that allows bifurcation analysis.

Nomenclature

E	=	Young's modulus
$\tilde{f}$	=	force excitation
h	=	shell thickness
k	=	stiffness of the rotational distributed springs
k_x, k_θ, $k_{x\theta}$	=	changes in curvature and torsion
L	=	shell length
m	=	number of axial half-waves
n	=	number of circumferential waves
R	=	shell radius
t	=	time
u	=	axial shell displacement
$u_{m,n,c}(t)$, $u_{m,n,s}(t)$	=	modal coordinates of axial displacement (time dependent)
v	=	circumferential shell displacement
$v_{m,n,c}(t)$, $v_{m,n,s}(t)$	=	modal coordinates of circumferential displacement (time dependent)
w	=	radial shell displacement
$w_{m,n,c}(t)$, $w_{m,n,s}(t)$	=	modal coordinates of radial displacement (time dependent)
w_0	=	radial geometric imperfection
x	=	longitudinal coordinate
ε_x, ε_θ, $\gamma_{x\theta}$	=	shell strains
$\varepsilon_{x,0}$, $\varepsilon_{\theta,0}$, $\gamma_{x\theta,0}$	=	middle surface strains
$\zeta_{1,n}$	=	modal damping coefficient of mode $(1, n)$
θ	=	angular coordinate
λ_m	=	$m\pi x/L$
ρ_S	=	mass density of the shell
Φ	=	velocity potential of fluid

I. Introduction

AN extensive review of studies on geometrically nonlinear (large-amplitude) vibrations of shells has been written recently by Amabili and Païdoussis.[1] From this review emerge the facts that the effect of boundary conditions on the nonlinear response of circular cylindrical shells is still not completely understood and that comparisons of results for different constraints are very scarce. In fact, most of the literature deals with simply supported shells. Not many studies on shells with different boundary conditions are available. In particular, Matsuzaki and Kobayashi[2] studied theoretically and experimentally large-amplitude vibrations of clamped circular cylindrical shells. They based their analysis on Donnell's nonlinear shallow-shell theory and used a simple mode expansion with two degrees of freedom. The analysis found a softening-type nonlinearity for clamped shells, in agreement with their own experimental results. They also found amplitude-modulated response close to resonance and identified it as a beating phenomenon due to frequencies very close to the excitation frequency.

Chia[3,4] studied nonlinear free vibrations and postbuckling of symmetrically and asymmetrically laminated circular cylindrical panels with imperfections and different boundary conditions. Donnell's nonlinear shallow-shell theory was used. A single-mode analysis was carried out, and the results showed a hardening nonlinearity. Iu and Chia[5] used Donnell's nonlinear shallow-shell theory to study free vibrations and postbuckling of clamped and simply supported, unsymmetrically laminated cross-ply circular cylindrical shells. A multimode expansion was used without considering a companion mode, and as a consequence only free vibrations were investigated. Radial geometric imperfections were taken into account. The homogeneous solution of the stress function was retained, but the dependence on the axial coordinate was neglected. The equations of motion were obtained by using the Galerkin method and were studied by harmonic balance. Three asymmetric and three axisymmetric modes were used in the numerical calculations. In a later paper, Fu and Chia[6] included in their model nonuniform boundary conditions around the edges. Softening- or hardening-type nonlinearities were found, depending on the radius-to-thickness ratio. Only undamped free vibrations and buckling were investigated in this series of studies.

Large-amplitude vibrations of two vertical clamped circular cylindrical shells, partially filled with water to different levels were experimentally studied by Chiba.[7] In this case, the responses displayed a general softening nonlinearity. The shells tested showed a larger nonlinearity when partially filled, as compared to the empty and completely filled cases. Large-amplitude vibrations of four axially loaded, clamped circular cylindrical shells made of aluminum were experimentally studied by Gunawan.[8]

Tsai and Palazotto[9] investigated the dynamic responses of circular cylindrical panels by developing a 36-degree-of-freedom, curved, quadrilateral, thin-shell finite element, incorporating large

Received 30 May 2002; revision received 15 December 2002; accepted for publication 18 December 2002.

*Associate Professor, Dipartimento di Ingegneria Industriale, Parco Area delle Scienze 181/A; marco@me.unipr.it.

displacement/rotation through the thickness and parabolic transverse shear strains.

Ganapathi and Varadan[10] used the finite element method to study large-amplitude vibrations of doubly curved composite shells. Numerical results are given for isotropic circular cylindrical shells. Only free vibrations were investigated, using Donnell's nonlinear kinematics for shell deformation. A four-node finite element was developed with five degrees of freedom for each node. Ganapathi and Varadan also pointed out problems in the finite element analysis of closed shells that are not present in open shells. The same approach was used to study numerically laminated composite circular cylindrical shells.[11]

On the other hand, the range of literature on large-amplitude vibrations of simply supported shells with and without fluid–structure interaction is much wider, for example, Refs. 12–17.

Circular cylindrical shells with different boundary conditions are investigated in the present study. In particular, simply supported shells with allowed and constrained axial displacements at the edges are studied; in both cases, the radial and circumferential displacements at the shell edges are constrained. Elastic rotational constraints at the shell ends are assumed; they allow simulating any condition from simply supported to perfectly clamped, by varying the stiffness of this elastic constraints.

The Lagrange equations of motion are obtained by an energy approach, retaining damping through Rayleigh's dissipation function. The formulation is also valid for orthotropic and symmetric cross-ply laminated composite shells and takes into account geometric imperfections. Comparison of calculations to experimental and numerical results available in the literature is also performed. Both empty and fluid-filled shells are investigated by using a potential fluid model. The nonlinear equations of motion are studied by using a code based on arclength continuation method that allows bifurcation analysis.

II. Elastic Strain Energy of the Shell

A circular cylindrical shell with the cylindrical coordinate system (O, x, r, θ), with O the origin at the center of one end of the shell, is shown in Fig. 1. The displacements of an arbitrary point of coordinates (x, θ) on the middle surface of the shell are denoted by u, v, and w in the axial, circumferential, and radial directions, respectively; w is taken positive outward. Initial imperfections of the circular cylindrical shell associated with zero initial tension are denoted by radial displacement w_0, also positive outward; only radial initial imperfections are considered.

Two different strain–displacement relationships for thin shells are used in the present study, to compare results. They are based on Love's first approximation assumptions: 1) the shell thickness h is small with respect to the radius of curvature R of the middle plane, 2) strains are small; 3) transverse normal stress is small, and 4) the Kirchhoff–Love kinematic hypothesis is used, in which it is assumed that the normal to the undeformed middle surface remains straight and normal to the midsurface after deformation, and undergoes no thickness stretching. These shell theories are 1) Donnell's (see Refs. 18 and 19) and 2) Novozhilov's[20] (also see Refs. 18 and 19) nonlinear shell theories. For both theories rotary inertia and shear deformations are neglected. In accord with to these two shell theories, the strain components ε_x, ε_θ, and $\gamma_{x\theta}$ at an arbitrary point of the shell are related to the middle surface strains $\varepsilon_{x,0}$, $\varepsilon_{\theta,0}$, and $\gamma_{x\theta,0}$ and to the changes in the curvature and torsion of the middle surface k_x, k_θ, and $k_{x\theta}$ by the following three relationships[18,19]:

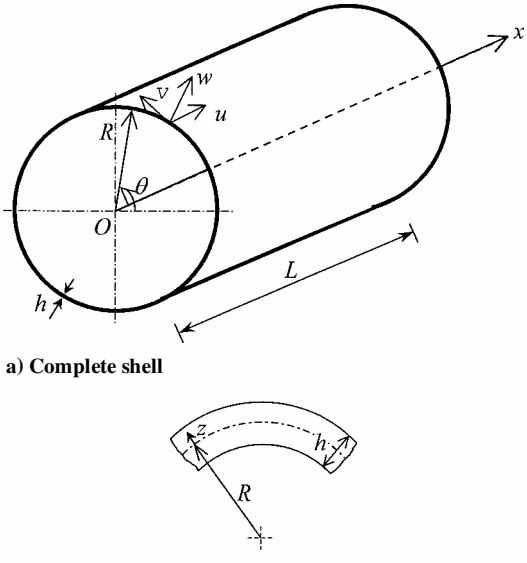

a) Complete shell

b) Cross section of the shell surface

Fig. 1 Circular cylindrical shell; coordinate system and dimensions.

$$\varepsilon_x = \varepsilon_{x,0} + zk_x \tag{1a}$$

$$\varepsilon_\theta = \varepsilon_{\theta,0} + zk_\theta \tag{1b}$$

$$\gamma_{x\theta} = \gamma_{x\theta,0} + zk_{x\theta} \tag{1c}$$

where z is the distance of the arbitrary point of the shell from the middle surface (Fig. 1b).

According to Donnell's nonlinear shell theory, the middle surface strain–displacement relationships and changes in the curvature and torsion are obtained for a circular cylindrical shell (see Ref. 18):

$$\varepsilon_{x,0} = \frac{\partial u}{\partial x} + \frac{1}{2}\left(\frac{\partial w}{\partial x}\right)^2 + \frac{\partial w}{\partial x}\frac{\partial w_0}{\partial x} \tag{2a}$$

$$\varepsilon_{\theta,0} = \frac{\partial v}{R\partial\theta} + \frac{w}{R} + \frac{1}{2}\left(\frac{\partial w}{R\partial\theta}\right)^2 + \frac{\partial w}{R\partial\theta}\frac{\partial w_0}{R\partial\theta} \tag{2b}$$

$$\gamma_{x\theta,0} = \frac{\partial u}{R\partial\theta} + \frac{\partial v}{\partial x} + \frac{\partial w}{\partial x}\frac{\partial w}{R\partial\theta} + \frac{\partial w}{\partial x}\frac{\partial w_0}{R\partial\theta} + \frac{\partial w_0}{\partial x}\frac{\partial w}{R\partial\theta} \tag{2c}$$

$$k_x = -\frac{\partial^2 w}{\partial x^2} \tag{2d}$$

$$k_\theta = -\frac{\partial^2 w}{R^2\partial\theta^2} \tag{2e}$$

$$k_{x\theta} = -2\frac{\partial^2 w}{R\partial x\partial\theta} \tag{2f}$$

According to Novozhilov's nonlinear theory,[20] displacements $\tilde{u}$, $\tilde{v}$, and $\tilde{w}$ of points at distance z from the middle surface are introduced; they are related to displacements on the middle surface by the relationships

$$\tilde{u} = u + z\theta \tag{3a}$$

$$\tilde{v} = v + z\psi \tag{3b}$$

$$\tilde{w} = w + w_0 + z\chi \tag{3c}$$

where

$$\theta = -\frac{\partial\,(w + w_0)}{\partial x}\left(1 + \frac{\partial v}{R\partial\theta} + \frac{w}{R}\right) + \left[\frac{\partial(w + w_0)}{R\partial\theta} - \frac{v}{R}\right]\frac{\partial u}{R\partial\theta} - \frac{\partial w}{\partial x}\frac{w_0}{R} \tag{3d}$$

$$\psi = -\left[\frac{\partial(w + w_0)}{R\partial\theta} - \frac{v}{R}\right]\left(1 + \frac{\partial u}{\partial x}\right) + \frac{\partial(w + w_0)}{\partial x}\frac{\partial v}{\partial x} \tag{3e}$$

$$\chi \cong \frac{\partial u}{\partial x} + \frac{\partial v}{R\partial\theta} + \frac{\partial u}{\partial x}\frac{\partial v}{R\partial\theta} - \frac{\partial u}{R\partial\theta}\frac{\partial v}{\partial x} \tag{3f}$$

The strain–displacement relationships for a generic point of the shell are

$$\varepsilon_x = \frac{\partial \tilde{u}}{\partial x} + \frac{1}{2}\left[\left(\frac{\partial \tilde{u}}{\partial x}\right)^2 + \left(\frac{\partial \tilde{v}}{\partial x}\right)^2 + \left(\frac{\partial \tilde{w}}{\partial x}\right)^2\right] \tag{4a}$$

$$\varepsilon_\theta = \frac{1}{R+z}\left(\frac{\partial \tilde{v}}{\partial \theta} + \tilde{w}\right) + \frac{1}{2(R+z)^2} \times \left[\left(\frac{\partial \tilde{u}}{\partial \theta}\right)^2 + \left(\frac{\partial \tilde{v}}{\partial \theta} + \tilde{w}\right)^2 + \left(\frac{\partial \tilde{w}}{\partial \theta} - \tilde{v}\right)^2\right] \tag{4b}$$

$$\gamma_{x\theta} = \frac{\partial \tilde{v}}{\partial x} + \frac{1}{R+z}\frac{\partial \tilde{u}}{\partial \theta} + \frac{1}{R+z} \times \left[\frac{\partial \tilde{u}}{\partial x}\frac{\partial \tilde{u}}{\partial \theta} + \frac{\partial \tilde{v}}{\partial x}\left(\frac{\partial \tilde{v}}{\partial \theta} + \tilde{w}\right) + \frac{\partial \tilde{w}}{\partial x}\left(\frac{\partial \tilde{w}}{\partial \theta} - \tilde{v}\right)\right] \tag{4c}$$

The following thinness approximations are now introduced:

$$1/(R+z) = 1/R\{1 - (z/R) + \mathcal{O}[(z/R)^2]\} \tag{5a}$$

$$1/(R+z)^2 = 1/R^2\{1 - (2z/R) + \mathcal{O}[(z/R)^2]\} \tag{5b}$$

where $\mathcal{O}[(z/R)^2]$ is a small quantity of order $(z/R)^2$. When Eqs. (3) are introduced into Eqs. (4) and approximations (5), the middle surface strain–displacement relationships, are used, changes in the curvature and torsion are obtained for the Novozhilov theory[20] of shells:

$$\varepsilon_{x,0} = \frac{\partial u}{\partial x} + \frac{1}{2}\left[\left(\frac{\partial u}{\partial x}\right)^2 + \left(\frac{\partial v}{\partial x}\right)^2 + \left(\frac{\partial w}{\partial x}\right)^2\right] + \frac{\partial w}{\partial x}\frac{\partial w_0}{\partial x} \tag{6a}$$

$$\varepsilon_{\theta,0} = \frac{\partial v}{R\partial \theta} + \frac{w}{R} + \frac{1}{2R^2}\left[\left(\frac{\partial u}{\partial \theta}\right)^2 + \left(\frac{\partial v}{\partial \theta} + w\right)^2 + \left(\frac{\partial w}{\partial \theta} - v\right)^2\right] + \frac{1}{R^2}\left[\frac{\partial w_0}{\partial \theta}\left(\frac{\partial w}{\partial \theta} - v\right) + w_0\left(w + \frac{\partial v}{\partial \theta}\right)\right] \tag{6b}$$

$$\gamma_{x\theta,0} = \frac{\partial v}{\partial x} + \frac{\partial u}{R\partial \theta} + \frac{1}{R}\left[\frac{\partial u}{\partial x}\frac{\partial u}{\partial \theta} + \frac{\partial v}{\partial x}\left(\frac{\partial v}{\partial \theta} + w\right) + \frac{\partial w}{\partial x}\left(\frac{\partial w}{\partial \theta} - v\right) + \frac{\partial w_0}{\partial x}\left(\frac{\partial w}{\partial \theta} - v\right) + \frac{\partial w}{\partial x}\frac{\partial w_0}{\partial \theta} + \frac{\partial v}{\partial x}w_0\right] \tag{6c}$$

$$k_x = -\frac{\partial^2 w}{\partial x^2} \tag{6d}$$

$$k_\theta = -\frac{\partial^2 w}{R^2\partial \theta^2} - \frac{w}{R^2} + \frac{\partial u}{R\partial x} + \frac{\partial v}{R^2\partial \theta} \tag{6e}$$

$$k_{x\theta} = -2\frac{\partial^2 w}{R\partial x\partial \theta} + \frac{\partial v}{R\partial x} - \frac{\partial u}{R^2\partial \theta} \tag{6f}$$

Equations (6a–6f) are an improved version of Novozhilov's nonlinear shell theory because approximations (5) have been used instead of neglecting terms in z and z^2 at this point of the derivation as was done in Ref. 20. Nonlinearities in changes of curvature and torsion have been neglected in this case for simplicity. The complete expression is given by Amabili.[17]

The elastic strain energy U_S of a circular cylindrical shell, neglecting σ_z as stated by Love's first approximation assumptions, is given by[19]

$$U_S = \frac{1}{2}\int_0^{2\pi}\int_0^L\int_{-h/2}^{h/2}(\sigma_x\varepsilon_x + \sigma_\theta\varepsilon_\theta + \tau_{x\theta}\gamma_{x\theta})\,\mathrm{d}x\,R\frac{1+z}{R}\,\mathrm{d}\theta\,\mathrm{d}z \tag{7}$$

where R is the shell middle radius and the stresses σ_x, σ_θ and $\tau_{x\theta}$ are related to the strain for homogeneous and isotropic material ($\sigma_z = 0$, case of plane stress) by[19]

$$\sigma_x = E/(1-\nu^2)(\varepsilon_x + \nu\varepsilon_\theta) \tag{8a}$$

$$\sigma_\theta = E/(1-\nu^2)(\varepsilon_\theta + \nu\varepsilon_x) \tag{8b}$$

$$\tau_{x\theta} = [E/2(1+\nu)]\gamma_{x\theta} \tag{8c}$$

where ν is the Poisson's ratio. When Eqs. (1), (7), and (8) are used, the following expression is obtained:

$$U_S = \frac{1}{2}\frac{Eh}{1-\nu^2}\int_0^{2\pi}\int_0^L\left(\varepsilon_{x,0}^2 + \varepsilon_{\theta,0}^2 + 2\nu\varepsilon_{x,0}\varepsilon_{\theta,0} + \frac{1-\nu}{2}\gamma_{x\theta,0}^2\right)\mathrm{d}x\,R\,\mathrm{d}\theta + \frac{1}{2}\frac{Eh^3}{12(1-\nu^2)} \times \int_0^{2\pi}\int_0^L\left(k_x^2 + k_\theta^2 + 2\nu\,k_xk_\theta + \frac{1-\nu}{2}k_{x\theta}^2\right)\mathrm{d}x\;R\,\mathrm{d}\theta + \frac{1}{2}\frac{Eh^3}{6R(1-\nu^2)}\int_0^{2\pi}\int_0^L\left(\varepsilon_{x,0}k_x + \varepsilon_{\theta,0}k_\theta + \nu\varepsilon_{x,0}k_\theta + \nu\varepsilon_{\theta,0}k_x + \frac{1-\nu}{2}\gamma_{x\theta,0}k_{x\theta}\right)\mathrm{d}x\,R\,\mathrm{d}\theta + \mathcal{O}(h^4) \tag{9}$$

where $\mathcal{O}(h^4)$ is a higher-order term in h and the last term in h^3 disappears if z/R is neglected with respect to unity in Eq. (7), as it must be done for Donnell's theory. If this term is neglected, the right-hand side of Eq. (9) can be easily interpreted: The first term is the membrane (also referred to as stretching) energy, and the second one is the bending energy. If the last term is retained, membrane and bending energies are coupled. In the Appendix, the expressions of the strain energy for orthotropic and symmetric cross-ply laminated composite shells are reported.

III. Mode Expansion, Kinetic Energy, and External Loads

The kinetic energy T_S of a circular cylindrical shell, by neglecting rotary inertia, is given by

$$T_S = \frac{1}{2}\rho_S h\int_0^{2\pi}\int_0^L(\dot{u}^2 + \dot{v}^2 + \dot{w}^2)\,\mathrm{d}x\,R\,\mathrm{d}\theta \tag{10}$$

In Eq. (10) the overdot denotes a time derivative.

The virtual work W done by the external forces is written as

$$W = \int_0^{2\pi}\int_0^L(q_x u + q_\theta v + q_r w)\,\mathrm{d}x\,R\,\mathrm{d}\theta \tag{11}$$

where q_x, q_θ, and q_r are the distributed forces per unit area acting in axial, circumferential, and radial directions, respectively. Initially, only a single harmonic radial force is considered; therefore $q_x = q_\theta = 0$. The external radial distributed load q_r applied to the shell, because of the radial concentrated force $\tilde{f}$, is given by

$$q_r = \tilde{f}\delta(R\theta - R\tilde{\theta})\delta(x - \tilde{x})\cos(\omega t) \tag{12}$$

where ω is the excitation frequency, t is the time, δ is the Dirac delta function, $\tilde{f}$ gives the radial force amplitude positive in the z direction, and $\tilde{x}$ and $\tilde{\theta}$ give the axial and angular positions of the point of application of the force, respectively. In the numerical calculations, the point excitation is located at $\tilde{x} = L/2$, $\tilde{\theta} = 0$. Equation (11) can be rewritten in the following form:

$$W = \tilde{f}\cos(\omega t)(w)_{x=L/2,\theta=0} \tag{13}$$

Equation (13) specialized for the expression of w used in the present study is given in Sec. V, together with the virtual work of axial loads and uniform radial pressure.

To reduce the system to finite dimensions, the middle surface displacements u, v, and w are expanded by using approximate functions. The following boundary conditions are imposed at the shell ends:

$$u = 0 \quad \text{at} \quad x = 0, L \tag{14a}$$

$$v = 0 \quad \text{at} \quad x = 0, L \tag{14b}$$

$$w = 0 \quad \text{at} \quad x = 0, L \tag{14c}$$

$$w_0 = 0 \quad \text{at} \quad x = 0, L \tag{14d}$$

$$M_x = -\frac{k\partial w}{\partial x} \quad \text{at} \quad x = 0, L \tag{14e}$$

$$\frac{\partial^2 w_0}{\partial x^2} = 0 \quad \text{at} \quad x = 0, L \tag{14f}$$

where M_x is the bending moment per unit length and k is the stiffness per unit length of the elastic, distributed rotational springs placed at $x = 0, L$. Moreover, u, v and w must be continuous in θ. The boundary conditions (14a–14c) restrain all of the shell displacements at both edges. Equation (14e) represents the case of an elastic rotational constraint at the shell edges. It gives any rotational constraint from zero moment ($M_x = 0$, unconstrained rotation) to perfectly clamped shell ($\partial w/\partial x = 0$, obtained as limit for $k \to \infty$), according to the value of k.

A base of shell displacements is used to discretize the system. In addition to the asymmetric mode directly driven into vibration by the excitation given in Eq. (12) (driven modes), it is necessary to consider 1) the orthogonal mode having the same shape and natural frequency but rotated by $\pi/(2n)$ (companion modes), 2) additional asymmetric modes, and 3) axisymmetric modes. In fact, it has clearly been established that, for large-amplitude shell vibrations, the deformation of the shell involves significant axisymmetric oscillations inward. In accord with these considerations, the displacements u, v, and w can be expanded by using the following expressions, which satisfy identically boundary conditions (14a–14c):

$$u(x,\theta,t) = \sum_{m=1}^{M_1}\sum_{j=1}^{N}[u_{m,j,c}(t)\cos(j\theta) + u_{m,j,s}(t)\sin(j\theta)] \times \sin(\lambda_m x) + \sum_{m=1}^{M_2} u_{m,0}(t)\sin(\lambda_m x) \tag{15a}$$

$$v(x,\theta,t) = \sum_{m=1}^{M_1}\sum_{j=1}^{N}[v_{m,j,c}(t)\sin(j\theta) + v_{m,j,s}(t)\cos(j\theta)] \times \sin(\lambda_m x) + \sum_{m=1}^{M_2} v_{m,0}(t)\sin(\lambda_m x) \tag{15b}$$

$$w(x,\theta,t) = \sum_{m=1}^{M_1}\sum_{j=1}^{N}[w_{m,j,c}(t)\cos(j\theta) + w_{m,j,s}(t)\sin(j\theta)] \times \sin(\lambda_m x) + \sum_{m=1}^{M_2} w_{m,0}(t)\sin(\lambda_m x) \tag{15c}$$

where j is the number of circumferential waves, m is the number of longitudinal half-waves, $\lambda_m = m\pi/L$, t is the time, and $u_{m,j}(t)$, $v_{m,j}(t)$, and $w_{m,j}(t)$ are the generalized coordinates that are unknown functions of t. The additional subscript c or s indicates if the generalized coordinate is associated to cos or sin function in θ, except for v, for which the notation is reversed (no additional subscript is used for axisymmetric terms). The integers N, M_1, and M_2 must be selected with care to obtain the required accuracy and acceptable dimension of the nonlinear problem.

Excitation in the neighborhood of resonance of mode with $m = 1$ longitudinal half-wave and n circumferential waves (mode with predominant radial oscillations), indicated as mode (m, n) for simplicity, is considered. The number of degrees of freedom that has been found to predict the nonlinear response with good accuracy is 54. This result is based on a convergence study similar to the one reported in Ref. 17 for simply supported shells. In particular, only modes with an odd m value of longitudinal half-waves can be considered for symmetry reasons in the expansions of v and w (if geometric imperfections with an even m value are not introduced); only even terms are necessary for u. Asymmetric modes having up to 12 longitudinal half-waves ($M_1 = M_2 = 12$) have been considered in the numerical calculations to achieve good accuracy. In fact, linear and nonlinear interaction among terms with different numbers of axial half-waves exists. In fact, these terms are not the linear modes of the shell with boundary conditions given by Eqs. (14). More terms are necessary for in-plane than for radial displacements.

The expansion used in the numerical calculation (Sec. VI) for excitation in the neighborhood of resonance of mode $(m = 1, n)$ is

$$u(x,\theta,t) = \sum_{m=1}^{6}[u_{2m,n,c}(t)\cos(n\theta) + u_{2m,n,s}(t)\sin(n\theta)]\cos(\lambda_{2m}x) + \sum_{m=1}^{6} u_{2m,0}(t)\cos(\lambda_{2m}x) + [u_{2,2n,c}(t)\cos(2n\theta) + u_{2,2n,s}(t)\sin(2n\theta)]\cos(\lambda_2 x) \tag{16a}$$

$$v(x,\theta,t) = \sum_{m=1}^{6}[v_{2m-1,n,c}(t)\sin(n\theta) + v_{2m-1,n,s}(t)\cos(n\theta)]\sin(\lambda_{2m-1}x) + [v_{1,2n,c}(t)\sin(2n\theta) + v_{1,2n,s}(t)\cos(2n\theta)]\sin(\lambda_1 x) + [v_{3,2n,c}(t)\sin(2n\theta) + v_{3,2n,s}(t)\cos(2n\theta)]\sin(\lambda_3 x) \tag{16b}$$

$$w(x,\theta,t) = \sum_{m=1}^{6}[w_{2m-1,n,c}(t)\cos(n\theta) + w_{2m-1,n,s}(t)\sin(n\theta)] \times \sin(\lambda_{2m-1}x) + \sum_{m=1}^{6} w_{2m-1,0}(t)\sin(\lambda_{2m-1}x) \tag{16c}$$

This expansion has 54 generalized coordinates (degrees of freedom) and guarantees good accuracy for the calculation performed in the present work, as numerically verified. The dimension of the nonlinear system is much smaller than 54 degrees of freedom, but a different base must be used to reduce the system. However, this base is very intuitive and allows calculations without loosing the physical significance of each term. Torsional axisymmetric terms are not necessary. Expansion (16) is an extension of the one developed for simply supported shells,[17] for which convergence has been highly investigated. In particular, more terms are necessary with respect to those used in Ref. 17 to have a good evaluation of the natural (linear) frequency because the functions used are different from the mode shape of the shell with constrained axial displacement ($u = 0$) at the shell ends. The addition of some extra terms, such as $u_{4,2n,c}(t)$ and $u_{4,2n,c}(t)$ has been checked numerically and does not give any significant change in the shell response.

The point excitation considered in Eq. (12) gives a direct excitation only to modes described by a cos function in angular direction, referred to as the driven modes, and to axisymmetric modes. The modes having the shape of the driven modes, but rotated by $\pi/(2n)$, that is, with form described by sin function in angular direction θ, are referred to as the companion modes.

A. Traveling Wave Response

The presence of couples of modes having the same shape but different angular orientations, the first one described by $\cos(n\theta)$ (driven mode) and the other by $\sin(n\theta)$ (companion mode), in the periodic response of the shell leads to the appearance of traveling wave vibration around the shell in the angular direction. This phenomenon is related to the axial symmetry of the system and is a fundamental difference vis-à-vis linear vibrations.

Away from resonance, the companion mode solution disappears $[u_{m,n,s}(t) = v_{m,n,s}(t) = w_{m,n,s}(t) = 0]$, and the generalized coordinates are nearly in phase or in opposite phase. The presence of the companion mode in the shell response leads to the appearance of a traveling wave and to more complex phase relationships among the generalized coordinates. The mode shapes are represented by Eq. (16). Let us consider for simplicity only radial motion, which is predominant for shells not particularly long. Suppose that the response of the driven and companion modes have the same frequency of oscillation of the excitation, that is, $w_{m,n,c}(t) = \bar{w}_{m,n,c}\cos(\omega t + \theta_1)$ and $w_{m,n,s}(t) = \bar{w}_{m,n,s}\cos(\omega t + \theta_2)$, and consider the other coordinates having smaller amplitude, then Eq. (16c) can be rearranged as

$$w = \sum_m \{[\bar{w}_{m,n,c}\cos(\omega t + \theta_1) + \bar{w}_{m,n,s}\sin(\omega t + \theta_2)]\cos(n\theta) + \bar{w}_{m,n,s}\sin(n\theta - \omega t - \theta_2)\}\sin\frac{m\pi x}{L} + \mathcal{O}\left(\bar{w}^2_{m,n,c}, \bar{w}^2_{m,n,s}, \bar{w}_{m,0}, \ldots\right) \tag{17}$$

where $\bar{w}_{m,n,c}$ and $\bar{w}_{m,n,s}$ are the amplitudes of driven and companion modes, respectively, θ_1 and θ_2 are the phases, and $\mathcal{O}$ is a small quantity. Equation (17) gives a combined solution consisting of a standing wave and a traveling wave of amplitude:

$$\sum_m \bar{w}_{m,n,s}$$

and moving in angular direction around the shell with angular velocity ω/n. The resulting standing wave is given by the sum of the two standing waves, one of amplitude

$$\sum_m \bar{w}_{m,n,c}$$

and the second of amplitude

$$\sum_m \bar{w}_{m,n,s}$$

with the same circular frequency ω and the same shape, but with a phase difference of $\theta_2 - \theta_1 - \pi/2$. When $\theta_2 - \theta_1 \cong \pi/2$, as is generally observed in calculations and experiments close to resonance, the amplitude of the resulting standing wave is almost

$$\sum_m (\bar{w}_{m,n,c} - \bar{w}_{m,n,s})$$

In contrast, in case of zero phase difference, that is, $\theta_2 - \theta_1 = 0$, no traveling wave arises.

B. Geometric Imperfections

Initial geometric imperfections of the circular cylindrical shell are considered only in radial direction. They are associated with zero initial stress. The radial imperfection w_0 is expanded in the same form of w, that is, in a double Fourier series satisfying the boundary conditions (14d) and (14f) at the shell edges:

$$w_0(x,\theta) = \sum_{m=1}^{\tilde{M}_1}\sum_{n=1}^{\tilde{N}}[A_{m,n}\cos(n\theta) + B_{m,n}\sin(n\theta)] \times \sin(\lambda_m x) + \sum_{m=1}^{\tilde{M}_2} A_{m,0}\sin(\lambda_m x) \tag{18}$$

where $A_{m,n}$, $B_{m,n}$, and $A_{m,0}$ are the modal amplitudes of imperfections; $\tilde{N}$, $\tilde{M}_1$, and $\tilde{M}_2$ are integers indicating the number of terms in the expansion. Equation (18) is the more general expression if zero imperfections are assumed at the shell ends. For computational purposes, only some of these terms can be introduced. It has been shown in Ref. 16 that geometric imperfections with n and $2n$ circumferential waves are the most important for the evaluation of the nonlinear response of modes with n circumferential waves.

C. Rotational Boundary Condition

Equations (14) give the boundary conditions. In particular, Eqs. (14a–14d) and (14f) are identically satisfied by the expansions of u, v, w, and w_0. Moreover, the continuity in θ of all of the displacement is also satisfied. On the other hand, Eqs. (14e) can be rewritten in the following form[19]:

$$M_x = \frac{Eh^3}{12(1-\nu^2)}(k_x + \nu k_\theta) = \frac{k\partial w}{\partial x} \qquad \text{at} \qquad x = 0, \quad L \tag{19}$$

In case of zero stiffness of the distributed rotational springs, $k = 0$, Eq. (19) is identically satisfied for the assumed expansion, according to the expressions of k_x and k_θ given in Eqs. (2d) and (2e) and Eqs. (6d) and (6e) for both Donnell's and Novozhilov's[20] nonlinear shell theories, respectively. In case of k different from zero, an additional potential energy stored by the elastic rotational springs at the shell edges must be added. This potential energy U_R is given by

$$U_R = \frac{1}{2}\int_0^{2\pi} k\left\{\left[\left(\frac{\partial w}{\partial x}\right)_{x=0}\right]^2 + \left[\left(\frac{\partial w}{\partial x}\right)_{x=L}\right]^2\right\}\mathrm{d}\theta \tag{20}$$

In Eq. (20) a nonuniform stiffness k (function of θ, simulating a nonuniform constraint) can be assumed.

To simulate clamped edges, corresponding to

$$\frac{\partial w}{\partial x} = 0 \qquad \text{at} \qquad x = 0, L \tag{21}$$

a very high value of the stiffness k must be assumed. In this case, Eq. (21) is satisfied by applying a condition on M_x; this approach is usually referred to as the artificial spring method,[21] and can be regarded as a variant of the classical penalty method. The values of the spring stiffness simulating a clamped shell can be obtained by trial and error or by evaluating the edge stiffness of the shell. In fact, it was found[22] that the natural frequencies of the system converge asymptotically to those of a clamped shell when k becomes very large.

IV. Fluid–Structure Interaction

The contained fluid is assumed to be incompressible and inviscid; these hypotheses turned out to be adequate for vibrations of water-filled shells.[16] The shell prestress due to the fluid weight is neglected. In the case numerically investigated in Sec. VI, this prestress is extremely small. The nonlinear effects in the dynamic pressure and in the boundary conditions at the fluid–structure interface are also neglected. These nonlinear effects have been found to be negligible by Gonçalves and Batista.[13] In fact, the amplitude of shell displacements remains small enough for linear fluid mechanics to be adequate. The fluid motion is described by the velocity potential Φ, which satisfies the Laplace equation,

$$\nabla^2\Phi = \frac{\partial^2\Phi}{\partial x^2} + \frac{\partial^2\Phi}{\partial r^2} + \frac{1}{r}\frac{\partial\Phi}{\partial r} + \frac{1}{r^2}\frac{\partial^2\Phi}{\partial\theta^2} = 0 \tag{22}$$

The fluid velocity vector $\boldsymbol{v}$ is related to Φ by $\boldsymbol{v} = -\nabla\Phi$. No cavitation is assumed at the fluid–shell interface:

$$\left(\frac{\partial\Phi}{\partial r}\right)_{r=R} = -\dot{w} \tag{23}$$

Both ends of the fluid volume (in correspondence to the shell edges) are assumed to be open, so that a zero pressure is assumed there:

$$(\Phi)_{x=0} = (\Phi)_{x=L} = 0 \tag{24}$$

A solution of Eq. (22) satisfying condition (24) is given by

$$\Phi = \sum_{m=1}^{\infty}\sum_{n=0}^{\infty}[\alpha_{mn}(t)\cos(n\theta) + \beta_{mn}(t)\sin(n\theta)] \times [c_{mn}I_n(\lambda_m r) + d_{mn}K_n(\lambda_m r)]\sin(\lambda_m x) \tag{25}$$

where $I_n(r)$ and $K_n(r)$ are the modified Bessel functions of the first and second kind, respectively, of order n and $\lambda_m = m\pi/L$. Equation (25) must satisfy boundary condition (23), and Φ must be finite (regular) at $r=0$. When the assumed mode expansion of w, given by Eq. (15c), is used, the solution of the boundary-value problem for internal fluid only is

$$\Phi = -\sum_{m=1}^{M}\sum_{n=0}^{N}[\dot{w}_{m,n,c}(t)\cos(n\theta) + \dot{w}_{m,n,s}(t)\sin(n\theta)] \times \frac{I_n(\lambda_m r)}{\lambda_m I_n'(\lambda_m R)}\sin(\lambda_m x) \tag{26}$$

where $I_n'(r)$ is the derivative of $I_n(r)$ with respect to its argument and M is the largest between M_1 and M_2, introduced in Eq. (15). Axisymmetric generalized coordinates are included with the subscript c for brevity. Therefore, the dynamic pressure p exerted by the contained fluid on the shell is given by

$$p = \rho_F(\dot{\Phi})_{r=R} = -\rho_F\sum_{m=1}^{M}\sum_{n=0}^{N}[\ddot{w}_{m,n,c}(t)\cos(n\theta) + \ddot{w}_{m,n,s}(t)\sin(n\theta)]\frac{I_n(\lambda_m R)}{\lambda_m I_n'(\lambda_m R)}\sin(\lambda_m x) \tag{27}$$

where ρ_F is the mass density of the internal fluid. Equation (27) shows that the fluid has an inertial effect on radial motion of the shell. In particular, the inertial effects are different for the asymmetric and the axisymmetric terms of the mode expansion. Hence, the fluid is expected to change the nonlinear behavior of the fluid-filled shell. Usually the inertial effect of the fluid is larger for axisymmetric modes, thus enhancing the nonlinear behavior of the shell.

Only kinetic energy T_F is associated to inviscid fluid without flow. When Green's theorem is used, this is given by

$$T_F = \frac{1}{2}\rho_F\int_0^{2\pi}\int_0^{L}(\Phi)_{r=R}\dot{w}\,\mathrm{d}x R\,\mathrm{d}\theta \tag{28}$$

V. Lagrange Equations of Motion

The nonconservative damping forces are assumed to be of viscous type and are taken into account by use of the Rayleigh's dissipation function

$$F = \frac{1}{2}c\int_0^{2\pi}\int_0^{L}(\dot{u}^2 + \dot{v}^2 + \dot{w}^2)\,\mathrm{d}x R\,\mathrm{d}\theta \tag{29}$$

where c has a different value for each term of the mode expansion. Simple calculations give

$$F = \frac{1}{2}\frac{L}{2}R\sum_{n=0}^{N}\sum_{m=1}^{M}\psi_n\left[c_{m,n,c}\left(\dot{u}_{m,n,c}^2 + \dot{v}_{m,n,c}^2 + \dot{w}_{m,n,c}^2\right) + c_{m,n,s}\left(\dot{u}_{m,n,s}^2 + \dot{v}_{m,n,s}^2 + \dot{w}_{m,n,s}^2\right)\right] \tag{30}$$

where

$$\psi_n = \begin{cases} 2\pi & \text{if} \quad n = 0 \\ \pi & \text{if} \quad n > 0 \end{cases} \tag{31}$$

The damping coefficient $c_{m,n,c\,\text{or}\,s}$ is related to the modal damping ratio, which can be evaluated from experiments, by $\zeta_{m,n,c\,\text{or}\,s} = c_{m,n,c\,\text{or}\,s}/(2\mu_{m,n}\omega_{m,n})$, where $\omega_{m,n}$ is the natural circular frequency of mode (m, n) and $\mu_{m,n}$ is the modal mass of this mode, given by $\mu_{m,n} = \psi_n(\rho_S + \rho_V)h(L/2)R$, and the virtual mass due to contained fluid is

$$\rho_V = \frac{\rho_F}{\lambda_m h}\frac{I_n(\lambda_m R)}{I_n'(\lambda_m R)} \tag{32}$$

The total kinetic energy of the system is

$$T = T_S + T_F \tag{33}$$

The potential energy of the system is given by the elastic strain energy of the shell and the energy stored by the two distributed rotational springs at the shell edges:

$$U = U_S + U_R \tag{34}$$

The virtual work done by the concentrated radial force $\tilde{f}$, expressed by Eq. (13), is specialized for the expression of w given in Eq. (15c):

$$W = \tilde{f}\cos(\omega t)(w)_{x=L/2,\theta=0} = \tilde{f}\cos(\omega t)\left[\sum_{m=1}^{M_1}\sum_{j=1}^{N}w_{m,j,c}(t) + \sum_{m=1}^{M_2}w_{m,0}(t)\right] \tag{35}$$

In presence of axial loads and radial pressure acting on the shell, additional virtual work is done by the external forces. In case of uniform internal time-varying pressure $p_r(t)$, the radial distributed force q_r is obviously

$$q_r = p_r(t) \tag{36}$$

The virtual work done by radial pressure is

$$W = \int_0^{2\pi}\int_0^{L}p_r(t)w\,\mathrm{d}x R\,\mathrm{d}\theta = 4Rp_r(t)L\sum_{m=1}^{M_2}\frac{w_{m,0}(t)}{m} \tag{37}$$

Equation (37) shows that only axisymmetric vibrations are directly excited by uniform radial pressure.

The following notation is introduced for brevity:

$$\boldsymbol{q} = \{u_{m,n,c}, u_{m,n,s}, v_{m,n,c}, v_{m,n,s}, w_{m,n,c}, w_{m,n,s}\}^T \qquad m = 1, \ldots, M, \qquad n = 0, \ldots, N \tag{38}$$

The generic element of the time-dependent vector $\boldsymbol{q}$ is referred to as q_j; the dimension of $\boldsymbol{q}$ is the number of degrees of freedom (DOF) used in the mode expansion.

The generalized forces Q_j are obtained by differentiation of Rayleigh's dissipation function and of the virtual work done by external forces:

$$Q_j = -\frac{\partial F}{\partial\dot{q}_j} + \frac{\partial W}{\partial q_j} = -c_{m,n,i,j,c/s}\dot{q}_j + \begin{cases} 0 & \text{if } q_j = u_{m,n,c/s},\ v_{m,n,c/s},\ \text{or } w_{m,n,s} \\ \tilde{f}\cos(\omega t) & \text{if } q_j = w_{m,n,c} \end{cases} \tag{39}$$

where the subscript c/s indicates c or s.

The Lagrange equations of motion for the fluid-filled shell are

$$\frac{\mathrm{d}}{\mathrm{d}t}\left(\frac{\partial T}{\partial\dot{q}_j}\right) - \frac{\partial T}{\partial q_j} + \frac{\partial U}{\partial q_j} = Q_j, \qquad j = 1, \ldots, \text{DOF} \tag{40}$$

where $\partial T/\partial q_j = 0$. These second-order equations have very long expressions containing quadratic and cubic nonlinear terms.

In particular,

$$\frac{\mathrm{d}}{\mathrm{d}t}\left(\frac{\partial T}{\partial \dot{q}_j}\right) = \begin{cases} \rho_S h(L/2)\psi_n R\ddot{q}_j & \text{if } q_j = u_{m,n,c/s} \text{ or } v_{m,n,c/s} \\ (\rho_S + \rho_V)h(L/2)\psi_n R\ddot{q}_j & \text{if } q_j = w_{m,n,c/s} \end{cases} \tag{41}$$

which shows that no inertial coupling exists in this case.

The very complicated term giving quadratic and cubic nonlinearities can be written in the form

$$\frac{\partial U}{\partial q_j} = \sum_{k=1}^{\mathrm{DOF}} q_k f_k + \sum_{i,k=1}^{\mathrm{DOF}} q_i q_k f_{i,k} + \sum_{i,k,l=1}^{\mathrm{DOF}} q_i q_k q_l f_{i,k,l} \tag{42}$$

where coefficients f have long expressions that also include geometric imperfections.

VI. Numerical Results

The equations of motion have been obtained by using Mathematica Ver. 4 computer software[23] for energy calculations to perform analytical surface integrals of trigonometric functions, for example, integrals in Eq. (9). The generic Lagrange equation j is divided by the modal mass associated with $\ddot{q}_j$ and then is transformed in two first-order equations. A nondimensionalization of variables is also performed for computational convenience: The frequencies are divided by the natural frequency $\omega_{m,n}$ of the mode (m, n) investigated, and the vibration amplitudes are divided by the shell thickness h. The resulting $2 \times \mathrm{DOF}$ equations are studied by 1) using AUTO 97 (Ref. 24) for continuation and bifurcation analysis of nonlinear ordinary differential equations and 2) direct integration of the equations of motion by using the DIVPAG routine of the FORTRAN library IMSL. AUTO 97 is capable of continuation of the solution, bifurcation analysis, and branch switching by using arclength continuation and collocation methods. In particular, the shell response under harmonic excitation has been studied by using an analysis in two steps: 1) First the excitation frequency was fixed far enough from resonance and the magnitude of the excitation was used as the bifurcation parameter; the solution was started at zero force, where the solution is the trivial undisturbed configuration of the shell, and was continued to reach the desired force magnitude. 2) When the desired magnitude of excitation was reached, the solution was continued by using the excitation frequency as the bifurcation parameter.

Calculations have been performed for a shell with the following dimensions and material properties: $L = 520$ mm, $R = 149.4$ mm, $h = 0.519$ mm, $E = 1.98 \times 10^{11}$ Pa, $\rho = 7800$ kg/m^3, and $\nu = 0.3$. This shell has fundamental mode with six circumferential waves and one longitudinal half-wave $(n = 6, m = 1)$ for boundary conditions given by Eqs. (14) for any stiffness k. The same shell, with simply supported edges, that is, with $k = 0$ and condition (14a) replaced by $N_x = 0$, where N_x is the axial force per unit length, has fundamental mode $(n = 5, m = 1)$. The shell is considered empty in Sec. VI.A and completely water filled in Sec. VI.B $(\rho_F = 1000$ kg/m$^3)$. In Sec. VI.C, numerical simulations are compared to experimental and numerical results reported by Matsuzaki and Kobayashi,[2] Chiba,[7] and Ganapathi and Varadan.[10]

A. Numerical Results for an Empty Shell

The nonlinear response of the empty shell in the spectral neighborhood of the fundamental frequency is shown in Fig. 2 for the shell with free rotation $(M_x = 0)$ and $u = 0$ at $x = 0$, L. The assumed modal damping is $\zeta_{1,n} = 0.001(\zeta_{1,n} = \zeta_{1,n,\mathrm{cors}})$. The fundamental mode $(n = 6, m = 1)$ has a natural frequency of 313.7 Hz according to the Flügge theory of shells with an expansion at convergence of the solution (60 longitudinal modes; computer code DIVA[22]). When expansion (16a–16c) is used, the natural frequency is 316.9 Hz for Donnell's theory and 309.9 Hz for Novozhilov's theory.[20] For the fundamental mode, the radial displacement w is largely predominant, and it is the only one shown. Only the most important generalized coordinate associated to driven and companion modes are presented in Fig. 2. However, the generalized coordinates associated

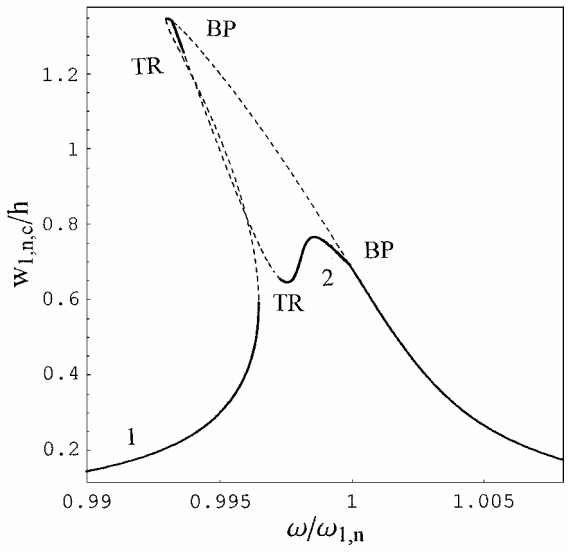

a) Amplitude of $w_{1,n,c}(t)$, driven mode

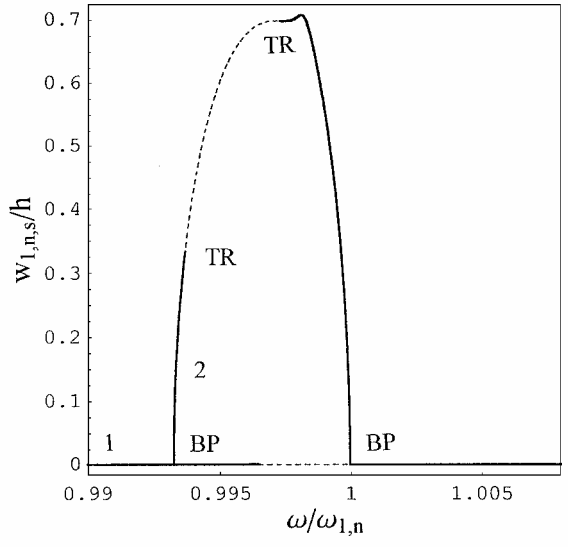

b) Amplitude of $w_{1,n,s}(t)$, companion mode

Fig. 2 Response amplitude–frequency relationship for the fundamental mode of the empty shell with free edge rotation (only simple periodic response), $\zeta_{1,n} = 0.001$, $\tilde{f} = 3$ N, and Donnell's theory: 1, branch 1; 2, branch 2; BP, pitchfork bifurcation; TR, Neimark–Sacher bifurcation; ——, stable response; and – – –, unstable response.

to terms with more longitudinal half-waves also make an important contribution to the shell response. Qualitatively, the generalized coordinate $w_{1,n,c}$, which is directly excited by the harmonic force $\tilde{f} = 3$ N, presents a branch 1, displaying a softening type nonlinearity, where branch 1 corresponds to zero companion mode participation $(w_{1,n,s} = 0)$. Branch 1 loses stability through a pitchfork bifurcation around the peak of the response. Through this bifurcation, branch 2 arises, which leads to companion mode participation. Branch 2 presents two Neimark–Sacher bifurcations (also defined as torus bifurcation); in between, the response is a stable two-periods quasiperiodic solution, that is, it presents amplitude modulations. (For this reason, the simple periodic response in Fig. 2 loses stability between the two Neimark–Sacher bifurcations). Figure 2 has been obtained by Donnell's theory (retaining in-plane inertia). Figure 3 shows the difference of branch 1 computed by using the more accurate Novozhilov's theory[20] and Donnell's theory. It is immediately observed that, for the thin shell investigated, the difference between the two theories is very small.

The same shell, but with clamped boundary conditions, is investigated in Fig. 4. The fundamental mode $(n = 6, m = 1)$ has a natural frequency of 315.1 Hz according to the Flügge theory of

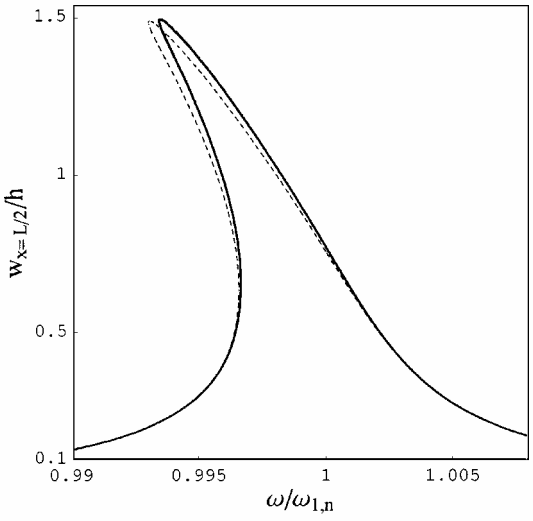

Fig. 3 Response amplitude–frequency relationship for the fundamental mode ($n=6$, $m=1$) of the empty shell with $u=0$ and free rotation, branch 1 only, $\zeta_{1,n}=0.001$, and $\tilde{f}=3$ N; shell displacement at the excitation point reported: – – –, Donnell's theory and ——, Novozhilov's theory.

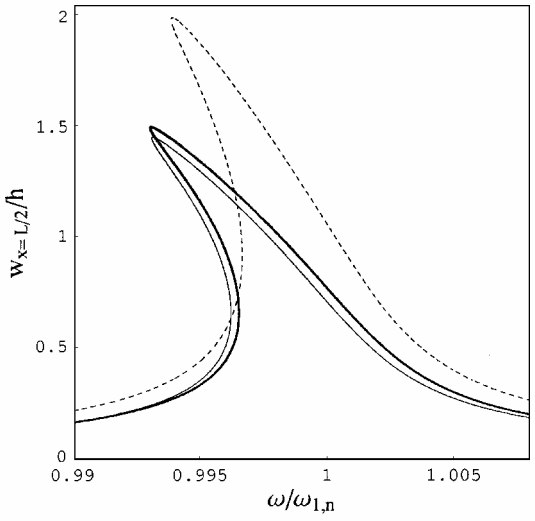

Fig. 5 Response amplitude–frequency relationship for the fundamental mode of the empty shell with different boundary conditions, branch 1 only, $\zeta_{1,n}=0.001$, and Donnell's theory; shell displacement at the excitation point reported: – – –, simply supported shell, ($n=5$, $m=1$), $\tilde{f}=2$ N; and ——, clamped shell, ($n=6$, $m=1$), $\tilde{f}=3$ N; and ——, shell with $u=0$ and free rotation, ($n=6$, $m=1$), $\tilde{f}=3$ N.

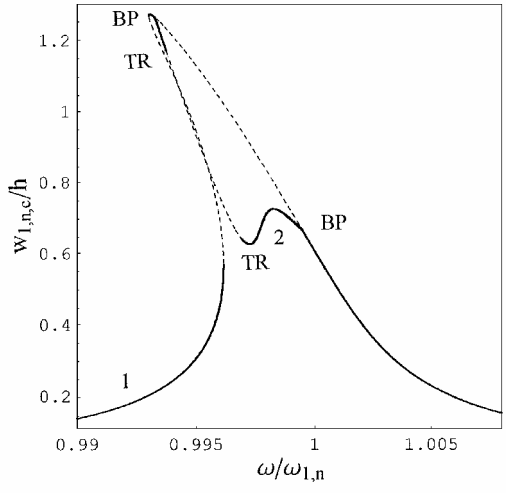

a) Amplitude of $w_{1,n,c}(t)$, driven mode

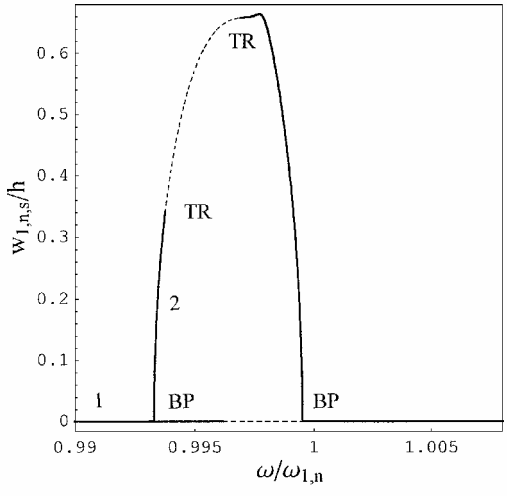

b) Amplitude of $w_{1,n,s}(t)$, companion mode

Fig. 4 Response amplitude–frequency relationship for the fundamental mode of the empty shell with clamped edges (only simple periodic response), $\zeta_{1,n}=0.001$, $\tilde{f}=3$ N, and Donnell's theory: 1, branch 1; 2, branch 2; BP, pitchfork bifurcation; TR, Neimark–Sacher bifurcation; ——, stable response; and – – –, unstable response.

shells with an expansion at convergence of the solution (60 longitudinal modes; computer code DIVA[22]). When expansion (16a–16c) is used, the natural frequency is 326.7 Hz with Donnell's theory. It can be easily observed that the natural frequency of the fundamental mode is very slightly increased by the rotational constraint with respect to the earlier case. In fact, the shell is very thin and sufficiently long to be little affected by this constraint, except in the two small regions close to the edges. The response–frequency relationship of the completely clamped shell is given in Fig. 4, and it is very close qualitatively and quantitatively to the one in Fig. 2. This is due to the small influence of the rotational constraint in this case.

A comparison of branch 1 of the responses in Figs. 2 and 4 to the one of the simply supported shell ($N_x=0$, $M_x=0$), for which the fundamental mode is ($n=5$, $m=1$) instead of ($n=6$, $m=1$), is provided in Fig. 5. The response of the simply supported shell has been taken from Amabili.[17] It is clearly shown that the axial constraint $u=0$ largely increases the softening-type nonlinearity of the shell with respect to the constraint $N_x=0$. (It can be also observed that the nonlinearity also increases with the number of circumferential waves n.)

The time response of the clamped shell for excitation frequency $\omega/\omega_{1,n}=0.9969$ and $\tilde{f}=3$ N is given in Fig. 6. (In this case, the response is in between the two Neimark–Sacher bifurcations.) It shows the two-period quasi-periodic (amplitude modulated) response described earlier. The Poincaré map for these conditions shows a closed loop, as shown in Ref. 25 for a simply supported shell, corresponding to a limit-cycle behavior. A frequency spectrum of the response shows some peaks close to the excitation frequency. Therefore, the modulations of amplitude are due to a beating phenomenon, and the solution is on a torus. In particular, a smaller time window is shown in Fig. 6d, and it is possible to observe a small phase difference between the driven ($w_{1,n,c}$) and the companion modes ($w_{1,n,s}$), whereas $w_{1,n,c}$ and $w_{3,n,c}$ are in phase. This phase difference indicates the beginning of a traveling wave around the shell superimposed on the standing wave.

B. Numerical Results for Water Filled Shell

The same clamped shell just investigated has been considered completely water filled with zero pressure at the shell ends. The response to harmonic excitation $\tilde{f}=3$ N in the neighborhood of the fundamental mode ($n=6$, $m=1$) is given in Fig. 7; it has been calculated assuming modal damping $\zeta_{1,n}=0.0017$. The natural frequency of the fundamental mode of the water-filled shell is 119.8 Hz according to the Flügge theory of shells with an expansion at convergence

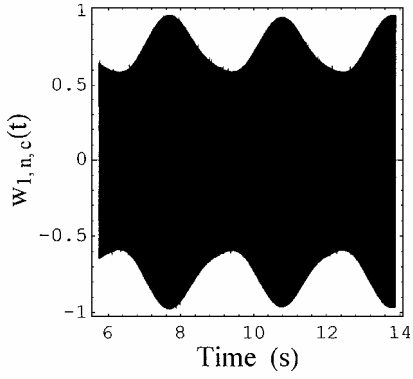

a) Generalized coordinate $w_{1,n,c}(t)$

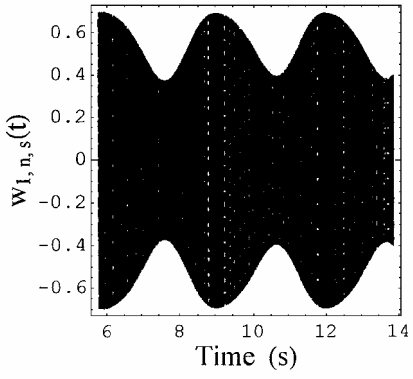

b) $w_{1,n,s}(t)$

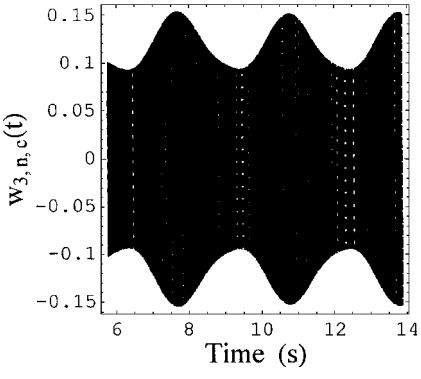

c) $w_{3,n,c}(t)$

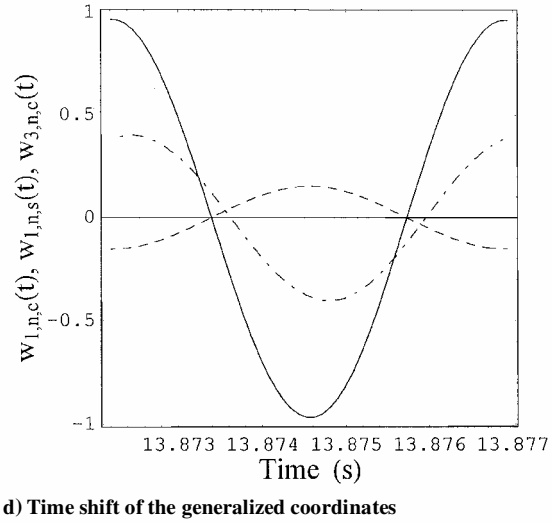

d) Time shift of the generalized coordinates

Fig. 6 Time response of the clamped shell in case of traveling wave response and amplitude modulations; $\omega/\omega_{1,n} = 0.999$, $\tilde{f} = 3$ N, mode ($n = 6$, $m = 1$), and Donnell's theory: ——, $w_{1,n,c}(t)$; – · –, $w_{1,n,s}(t)$; and – – –, $w_{3,n,c}(t)$.

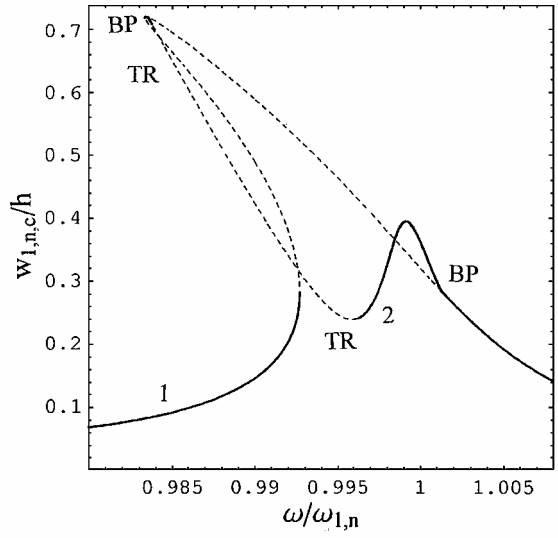

a) Amplitude of $w_{1,n,c}(t)$, driven mode

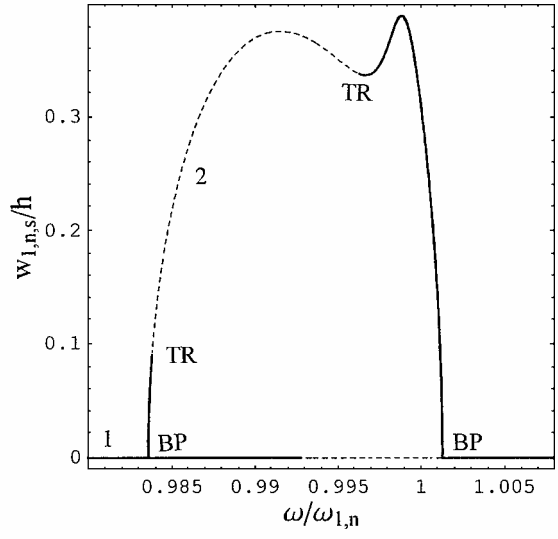

b) Amplitude of $w_{1,n,s}(t)$, companion mode

Fig. 7 Response amplitude–frequency relationship for the fundamental mode of the water-filled shell (only simple periodic response), $\zeta_{1,n} = 0.0017$, $\tilde{f} = 3$ N, and Donnell's theory: 1, branch 1; 2, branch 2; BP, pitchfork bifurcation; TR, Neimark–Sacher bifurcation; ——, stable response; and – – –, unstable response.

of the solution (60 longitudinal modes, $k = 10^{10}$ N, and computer code DIVA[22]). When expansion (16a–16c), $k = 10^{10}$ N, and Donnell's theory are used, the natural frequency is 124.3 Hz, with a difference of 3.6%.

Even if the vibration amplitude is still below the shell thickness, significant softening-type nonlinearity is observed in Fig. 7. A comparison of Figs. 4 and 7 shows that the presence of dense fluid enhances the shell nonlinearity. Moreover, in the frequency region around $\omega/\omega_{1,n} = 0.995$ (finishing at the right-hand Neimark–Sacher bifurcation), no stable solutions are indicated in Fig. 7. In this frequency region, there is a two-period quasi-periodic response, with amplitude modulations.

C. Comparison with Numerical and Experimental Results Available for Empty Shells

A first comparison has been performed for a clamped polyester shell, experimentally tested by Chiba,[7] with the following dimensions and material properties: $L = 480$ mm, $R = 240$ mm, $h = 0.254$ mm, $E = 4.65 \times 10^9$ Pa, $\rho = 1400$ kg/m^3, and $\nu = 0.38$. As a consequence of the circular cylindrical shell having a longitudinal lap-joint seam, the axial symmetry of the shell was broken, and the measured response of the vibration mode ($n = 15$,

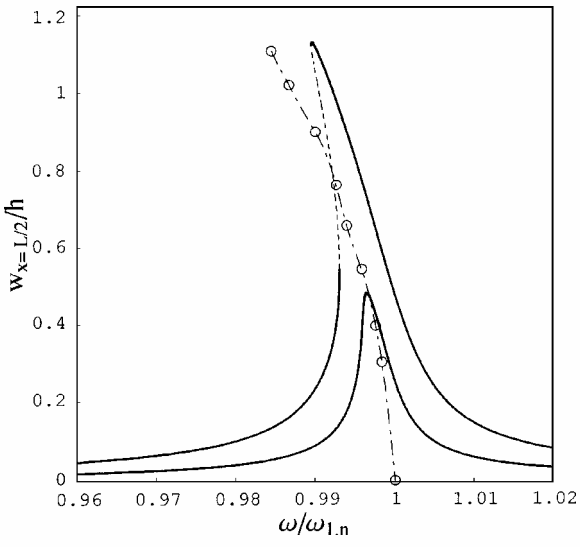

Fig. 8 Response amplitude–frequency relationship for mode ($n = 15$, $m = 1$) of the empty shell experimentally tested by Chiba[7] for two force levels, $\tilde{f} = 0.008$ N and $\tilde{f} = 0.02$ N, branch 1 only, $\zeta_{1,n} = 0.0015$, and Donnell's theory; shell displacement at excitation point $x = L/2$ reported: ——, theoretical stable response; – – –, theoretical unstable response; ○, experimental result from Ref. 7; and – · –, backbone curve fitting the experimental results.

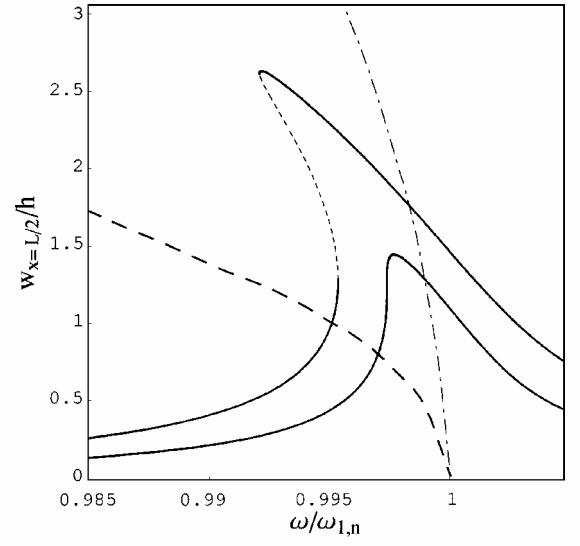

Fig. 9 Response amplitude–frequency relationship for mode ($n = 8$, $m = 1$) of the empty shell studied by Matsuzaki and Kobayashi[2] and Ganapathi and Varadan[10] for two force levels, $\tilde{f} = 0.025$ N and $\tilde{f} = 0.048$ N, branch 1 only, $\zeta_{1,n} = 0.0015$, and Donnell's theory; shell displacement at excitation point $x = L/2$ reported: ——, theoretical stable response; – – –, theoretical unstable response; ▬▬, backbone curve from Ref. 2; and – · –, backbone curve from Ref. 10.

$m = 1$) did not present a traveling wave. For this reason, the companion mode was eliminated by the expansion of the shell displacements in the numerical calculation of this case. The natural frequency of mode ($n = 15$, $m = 1$) is 95.7 Hz, according to Donnell's shell theory; $k = 10^8$ N has been assumed, which is large enough to simulate clamped ends in this case. The numerical response, evaluated for two force levels $\tilde{f} = 0.008$ and 0.02 N and modal damping $\zeta_{1,n} = 0.0015$, is plotted in Fig. 8 and is compared to the backbone curve (giving the free-vibration resonance, corresponding to the maximum of the response vs the vibration amplitude) obtained by Chiba.[7] Figure 8 shows the same trend of softening-type nonlinearity computed by using the present approach and the experimental results obtained by Chiba,[7] but some quantitative difference is present for the larger of the two excitations.

A second comparison has been performed with the numerical simulations of Matsuzaki and Kobayashi[2] and Ganapathi and Varada,[10] both of them for the fundamental mode ($n = 8$, $m = 1$) of the following clamped shell made of superinvar: $L = 110$ mm, $R = 55$ mm, $h = 0.052$ mm, $E = 125.6 \times 10^9$ Pa, $\rho = 7975.5$ kg/m^3, and $\nu = 0.25$. The natural frequency of the fundamental mode is 888.2 Hz, according to Donnell's shell theory; $k = 10^6$ N has been assumed, which is large enough to simulate clamped ends in this case. The numerical response (branch 1 only), evaluated for two force levels $\tilde{f} = 0.025$ and 0.048 N and modal damping $\zeta_{1,n} = 0.0015$, is plotted in Fig. 9 and compared to the backbone curves of Matsuzaki and Kobayashi[2] and Ganapathi and Varadan.[10] A large difference is observed between the results of Matsuzaki and Kobayashi[2] and Ganapathi and Varadan.[10] Differences among different studies justify the effort for new research on nonlinear dynamics of shells. Present results fall between those of Refs. 2 and 10 but are closer to those of Ganapathi and Varadan.[10]

VII. Conclusions

A flexible energy approach has been developed to study nonlinear vibrations of thin circular shells. It has been used with two different, nonlinear, thin shell theories. The method is suitable to model different boundary conditions via elastic constraints. Results show that circular cylindrical shells with restrained axial displacement at the shell edges display significantly stronger softening-type nonlinearity than simply supported shells. On the other hand, the rotational constraint has a small effect on the nonlinearity of very thin shells. The nonlinearity is enhanced for a completely water-filled shell with respect to the same empty shell. Numerical results are compared to those available in the literature.

Appendix: Strain Energy for Orthotropic and Symmetric Cross-Ply Laminated Composite Shells

When Love's first approximation assumptions are applied, the stresses σ_x, σ_θ, and $\tau_{x\theta}$ are related to the strain for orthotropic homogeneous material by[26]

$$\sigma_x = E_x/(1 - \nu_{x\theta}\nu_{\theta x})(\varepsilon_x + \nu_{\theta x}\,\varepsilon_\theta) \tag{A1a}$$

$$\sigma_\theta = E_\theta/(1 - \nu_{x\theta}\nu_{\theta x})(\varepsilon_\theta + \nu_{x\theta}\varepsilon_x) \tag{A1b}$$

$$\tau_{x\theta} = G_{x\theta}\gamma_{x\theta} \tag{A1c}$$

where E_x and E_θ are Young's moduli in the x and θ directions, respectively, $\nu_{x\theta}$ and $\nu_{x\theta}$ are Poisson's ratios, and $G_{x\theta}$ is the shear

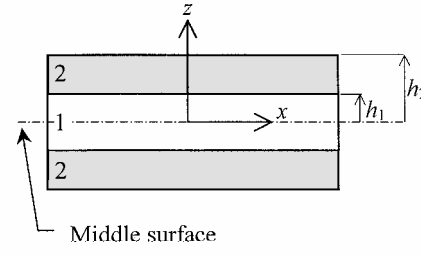

a) Shell with odd number of laminas

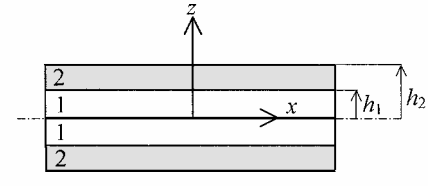

b) Shell with even number of laminas

Fig. A1 Symmetric laminated composite shell, distance h_j of the upper surface of the j lamina from the middle surface of the shell and numeration of layers of half-laminate.

modulus. The following relationship exists between Poisson's ratios and Young's moduli[26]:

$$\nu_{\theta x} E_x = \nu_{x\theta} E_\theta \tag{A2}$$

When Eqs. (7), (A1), and (A2) are used, the following expression for the strain energy of orthotropic shells is obtained:

$$\begin{aligned} U_S = {} & \frac{1}{2}\frac{E_x h}{1-\nu_{\theta x}^2 E_x/E_\theta}\int_0^{2\pi}\int_0^L \left[\varepsilon_{x,0}^2 + \frac{E_\theta}{E_x}\varepsilon_{\theta,0}^2 + 2\nu_{\theta x}\varepsilon_{x,0}\varepsilon_{\theta,0}\right. \\ & \left. + \frac{G_{x\theta}}{E_x}\frac{1-\nu_{\theta x}^2 E_x}{E_\theta}\gamma_{x\theta,0}^2\right] \mathrm{d}x\, R\, \mathrm{d}\theta \\ & + \frac{1}{2}\frac{E_x h^3}{12\left(1-\nu_{\theta x}^2 E_x/E_\theta\right)}\int_0^{2\pi}\int_0^L \left[k_x^2 + \frac{E_\theta}{E_x}k_\theta^2 + 2\nu_{\theta x}k_x k_\theta\right. \\ & \left. + \frac{G_{x\theta}}{E_x}\frac{1-\nu_{\theta x}^2 E_x}{E_\theta}k_{x\theta}^2\right] \mathrm{d}x\, R\, \mathrm{d}\theta + \frac{1}{2}\frac{E_x h^3}{6R\left(1-\nu_{\theta x}^2 E_x/E_\theta\right)} \\ & \times \int_0^{2\pi}\int_0^L \left[\varepsilon_{x,0}k_x + \frac{E_\theta}{E_x}\varepsilon_{\theta,0}k_\theta + \nu_{\theta x}\varepsilon_{x,0}k_\theta + \nu_{\theta x}\varepsilon_{\theta,0}k_x\right. \\ & \left. + \frac{G_{x\theta}}{E_x}\frac{1-\nu_{\theta x}^2 E_x}{E_\theta}\gamma_{x\theta,0}k_{x\theta}\right] \mathrm{d}x\, R\, \mathrm{d}\theta \end{aligned} \tag{A3}$$

Now the attention is focused on symmetric, laminated composite shells. A laminate is called symmetric when for each layer on one side of the middle surface there is a corresponding identical layer on the other side. It is assumed that each lamina is orthotropic and that each lamina's orthotropic principal directions coincide with the shell coordinates; this kind of laminate is referred as symmetric cross-ply laminate. It is convenient to introduce the distance h_j of the upper surface of the j lamina from the middle surface of the shell (Fig. A1), where $j = 1, \ldots H$, and H is the total number of layers of the half-laminate. (The central half-lamina in a laminate with odd number of layers counts for one.) For a laminate with an even number of laminas, the first surface of the half-laminate coincides with the middle surface of the shell and is not considered. The expression of the strain energy for this laminated composite shell is obtained as a generalization of Eq. (A3):

$$\begin{aligned} U_S = {} & \sum_{j=1}^{H}\frac{E_{x_j}(h_j - h_{j-1})}{1-\nu_{\theta x_j}^2 E_{x_j}/E_{\theta_j}}\int_0^{2\pi}\int_0^L \left[\varepsilon_{x,0}^2 + \frac{E_{\theta_j}}{E_{x_j}}\varepsilon_{\theta,0}^2\right. \\ & \left. + 2\nu_{\theta x_j}\varepsilon_{x,0}\varepsilon_{\theta,0} + \frac{G_{x\theta_j}}{E_{x_j}}\left(1-\nu_{\theta x_j}^2\frac{E_{x_j}}{E_{\theta_j}}\right)\gamma_{x\theta,0}^2\right] \mathrm{d}x\, R\, \mathrm{d}\theta \\ & + \sum_{j=1}^{H}\frac{E_{x_j}\left(h_j^3 - h_{j-1}^3\right)}{3\left(1-\nu_{\theta x_j}^2 E_{x_j}/E_{\theta_j}\right)}\int_0^{2\pi}\int_0^L \left[k_x^2 + \frac{E_{\theta_j}}{E_{x_j}}k_\theta^2\right. \\ & \left. + 2\nu_{\theta x_j}k_x k_\theta + \frac{G_{x\theta_j}}{E_{x_j}}\left(1-\nu_{\theta x_j}^2\frac{E_{x_j}}{E_{\theta_j}}\right)k_{x\theta}^2\right] \mathrm{d}x\, R\, \mathrm{d}\theta \\ & + \sum_{j=1}^{H}\frac{2E_{x_j}\left(h_j^3 - h_{j-1}^3\right)}{3R\left(1-\nu_{\theta x_j}^2 E_{x_j}/E_{\theta_j}\right)}\int_0^{2\pi}\int_0^L \left[\varepsilon_{x,0}k_x\right. \\ & + \frac{E_{\theta_j}}{E_{x_j}}\varepsilon_{\theta,0}k_\theta + \nu_{\theta x_j}\varepsilon_{x,0}k_\theta + \nu_{\theta x_j}\varepsilon_{\theta,0}k_x \\ & \left. + \frac{G_{x\theta_j}}{E_{x_j}}\left(1-\nu_{\theta x_j}^2\frac{E_{x_j}}{E_{\theta_j}}\right)\gamma_{x\theta,0}k_{x\theta}\right] \mathrm{d}x\, R\, \mathrm{d}\theta \end{aligned} \tag{A4}$$

where $h_0 = 0$ and the subscript j refers to the material properties of the j lamina. Equation (A4) is under Love's first approximation assumptions.

Acknowledgment

This work was partially supported by a FIRB grant (2001) of the Italian Ministry for University and Research.

References

[1]Amabili, M., and Païdoussis, M. P., "Review of Studies on Geometrically Nonlinear Vibrations and Dynamics of Circular Cylindrical Shells and Panels, with and Without Fluid–Structure Interaction," *Applied Mechanics Reviews* (to be published).

[2]Matsuzaki, Y., and Kobayashi, S., "A Theoretical and Experimental Study of the Nonlinear Flexural Vibration of Thin Circular Cylindrical Shells with Clamped Ends," *Transactions of the Japan Society for Aeronautical and Space Sciences*, Vol. 12, 1969, pp. 55–62.

[3]Chia, C. Y., "Non-Linear Free Vibration and Postbuckling of Symmetrically Laminated Orthotropic Imperfect Shallow Cylindrical Panels with Two Adjacent Edges Simply Supported and the Other Edges Clamped," *International Journal of Solids and Structures*, Vol. 23, 1987, pp. 1123–1132.

[4]Chia, C. Y., "Nonlinear Vibration and Postbuckling of Unsymmetrically Laminated Imperfect Shallow Cylindrical Panels with Mixed Boundary Conditions Resting on Elastic Foundation," *International Journal of Engineering Sciences*, Vol. 25, 1987, pp. 427–441.

[5]Iu, V. P., and Chia, C. Y., "Non-Linear Vibration and Postbuckling of Unsymmetric Cross-Ply Circular Cylindrical Shells," *International Journal of Solid Structures*, Vol. 24, 1988, pp. 195–210.

[6]Fu, Y. M., and Chia, C. Y., "Non-Linear Vibration and Postbuckling of Generally Laminated Circular Cylindrical Thick Shells with Non-Uniform Boundary Conditions," *International Journal of Non-Linear Mechanics*, Vol. 28, 1993, pp. 313–327.

[7]Chiba, M., "Experimental Studies on a Nonlinear Hydroelastic Vibration of a Clamped Cylindrical Tank Partially Filled with Liquid," *Journal of Pressure Vessel Technology*, Vol. 115, 1993, pp. 381–388.

[8]Gunawan, L., "Experimental Study of Nonlinear Vibrations of Thin-Walled Cylindrical Shells," Ph.D. Dissertation, Faculty of Aerospace Engineering, Technische Univ. Delft, Delft, The Netherlands, April 1998.

[9]Tsai, C. T., and Palazotto, A. N., "On the Finite Element Analysis of Non-Linear Vibration for Cylindrical Shells with High-Order Shear Deformation Theory," *International Journal of Non-Linear Mechanics*, Vol. 26, 1991, pp. 379–388.

[10]Ganapathi, M., and Varadan, T. K., "Large-Amplitude Vibrations of Circular Cylindrical Shells," *Journal of Sound and Vibration*, Vol. 192, 1996, pp. 1–14.

[11]Ganapathi, M., and Varadan, T. K., "Nonlinear Free Flexural Vibrations of Laminated Circular Cylindrical Shells," *Composite Structures*, Vol. 30, 1995, pp. 33–49.

[12]Dowell, E. H., and Ventres, C. S., "Modal Equations for the Nonlinear Flexural Vibrations of a Cylindrical Shell," *International Journal of Solids and Structures*, Vol. 4, 1968, pp. 975–991.

[13]Gonçalves, P. B., and Batista, R. C., "Non-Linear Vibration Analysis of Fluid-Filled Cylindrical Shells," *Journal of Sound and Vibration*, Vol. 127, 1988, pp. 133–143.

[14]Kobayashi, Y., and Leissa, A. W., "Large-Amplitude Free Vibration of Thick Shallow Shells Supported by Shear Diaphragms," *International Journal of Non-Linear Mechanics*, Vol. 30, 1995, pp. 57–66.

[15]Amabili, M., Pellicano, F., and Païdoussis, M. P., "Non-Linear Dynamics and Stability of Circular Cylindrical Shells Containing Flowing Fluid. Part I: Stability," *Journal of Sound and Vibration*, Vol. 225, 1999, pp. 655–699.

[16]Amabili, M., "Theory and Experiments for Large-Amplitude Vibrations of Empty and Fluid-Filled Circular Cylindrical Shells with Imperfections," *Journal of Sound and Vibration*, Vol. 262, No. 4, 2003, pp. 921–975.

[17]Amabili, M., "Comparison of Different Shell Theories for Large-Amplitude Vibrations of Empty and Fluid-Filled Circular Cylindrical Shells with and without Imperfections: Lagrangian Approach," *Journal of Sound and Vibration* (to be published).

[18]Yamaki, N., *Elastic Stability of Circular Cylindrical Shells*, North-Holland, Amsterdam, 1984.

[19]Leissa, A. W., *Vibration of Shells*, NASA SP-288, 1973; also available from the Acoustical Society of America, Melville, NY, 1993.

[20]Novozhilov, V. V., *Foundations of the Nonlinear Theory of Elasticity*, Graylock Press, Rochester, NY, 1953.

[21] Yuan, J., and Dickinson, S. M., "On the Use of Artificial Springs in the Study of the Free Vibrations of Systems Comprised of Straight and Curved Beams," *Journal of Sound and Vibration*, Vol. 152, 1992, pp. 203–216.

[22] Amabili, M., and Garziera, R., "Vibrations of Circular Cylindrical Shells with Nonuniform Constraints, Elastic Bed and Added Mass; Part I: Empty and Fluid-Filled Shells," *Journal of Fluids and Structures*, Vol. 14, 2000, pp. 669–690.

[23] Wolfram, S., *The Mathematica Book*, 4th ed., Cambridge Univ. Press, Cambridge, England, U.K., 1999.

[24] Doedel, E. J., Champneys, A. R., Fairgrieve, T. F., Kuznetsov, Y. A., Sandstede, B., and Wang, X., "AUTO 97: Continuation and Bifurcation Software for Ordinary Differential Equations (with HomCont)," Concordia Univ., Montreal, 1998.

[25] Amabili, M., Pellicano, F., and Païdoussis, M. P., "Non-Linear Dynamics and Stability of Circular Cylindrical Shells Containing Flowing Fluid. Part III: Truncation Effect Without Flow and Experiments," *Journal of Sound and Vibration*, Vol. 237, 2000, pp. 617–640.

[26] Daniel, I. M., and Ishai, O., *Engineering Mechanics of Composite Materials*, Oxford Univ. Press, New York, 1994.

C. Pierre
Associate Editor